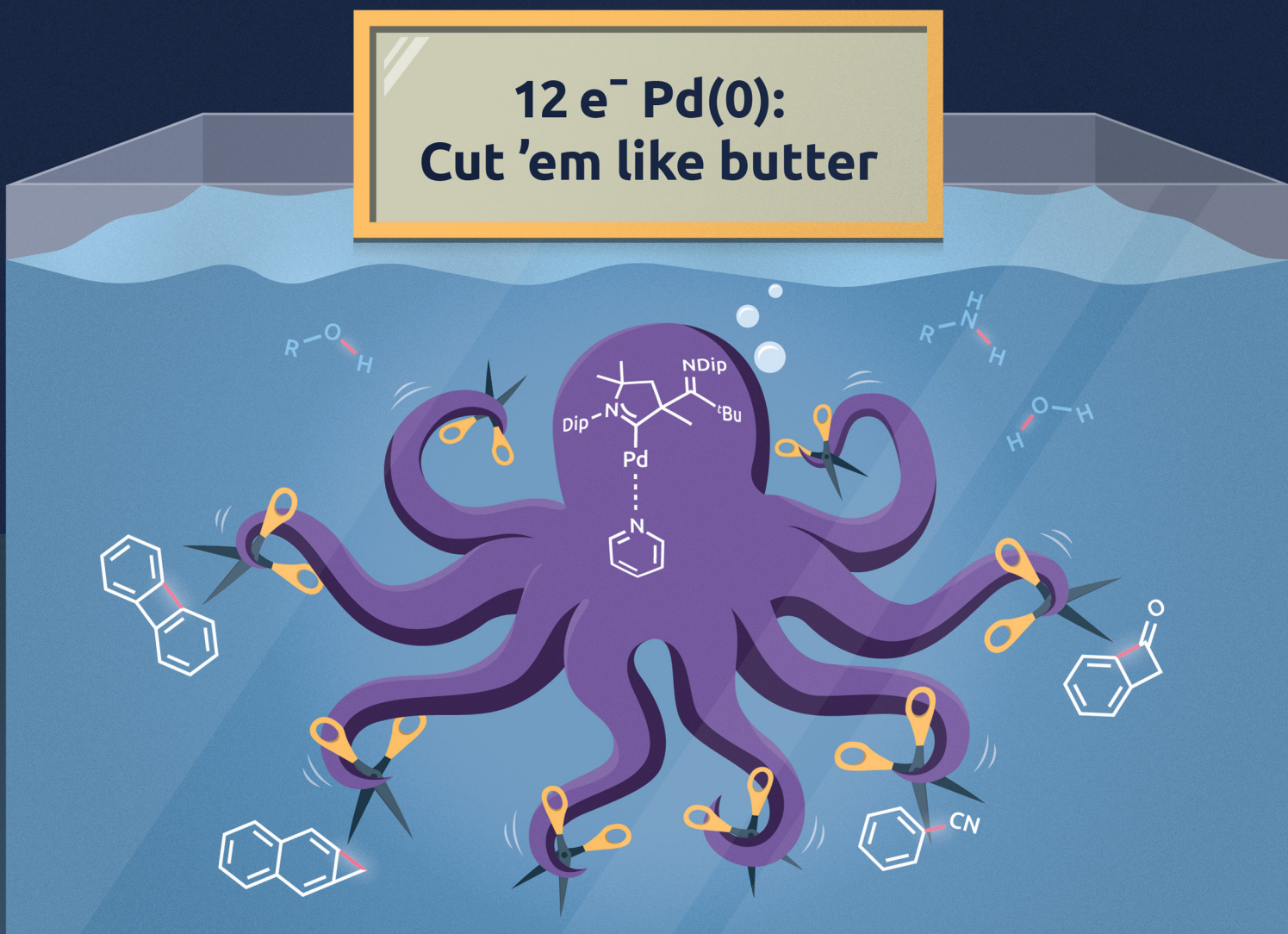


# ChemComm

Chemical Communications

rsc.li/chemcomm

## 12 e<sup>-</sup> Pd(0): Cut 'em like butter



ISSN 1359-7345



# Swift C–C bond insertion by a 12-electron palladium(0) surrogate†

 Kevin Breitwieser,<sup>id</sup><sup>a</sup> Fabian Dankert,<sup>id</sup><sup>a</sup> Annette Grünwald,<sup>ab</sup> Paula R. Mayer,<sup>a</sup> Frank W. Heinemann<sup>id</sup><sup>b</sup> and Dominik Munz<sup>id</sup><sup>\*ab</sup>

 Cite this: *Chem. Commun.*, 2023, 59, 12104

 Received 16th August 2023,  
 Accepted 14th September 2023

DOI: 10.1039/d3cc03964a

rsc.li/chemcomm

The selective activation of C–C bonds holds vast promise for catalysis. So far, research has been primarily directed at rhodium and nickel under harsh reaction conditions. Herein, we report C–C insertion reactions of a 12-electron palladium(0) surrogate stabilized by a cyclic(alkyl)(amino) carbene (CAAC) ligand. Benzonitrile (1), biphenylene (2), benzocyclobutenone (3), and naphtho[*b*]cyclopropene (4) were studied. These substrates allow elucidation of the effect of ring strain as well as hybridization encompassing sp<sup>3</sup>, sp<sup>2</sup> and sp hybridized carbon atoms. All reactions proceed quantitatively at or below room temperature. This work therefore outlines perspectives for mild C–C bond functionalization catalysis.

The functionalization of C–C bonds allows for the modification of organic molecules without the requirement for specific functional groups.<sup>1</sup> However, the elegance of this reaction-type is compromised by the strong and sterically shielded C–C bond, which renders the insertion step difficult. The most common transition metals used for catalytic transformations of C–C bonds are arguably rhodium and nickel. This is exemplified by the Rh-catalyzed cyclobutene ring opening<sup>2</sup> and the Ni-catalyzed transfer hydrocyanation.<sup>3</sup> However, also here, harsh reaction conditions, namely refluxing toluene or xylene solvents, are needed to break the C–C bond. These reactions may even take several days if not weeks to achieve high conversions.<sup>4,5</sup> As such, mild pathways to isolable, yet strained group-10 metallacycles are scarce as highlighted by Moret *et al.* for a nickelacyclobutane.<sup>6</sup>

So far, only a handful of C–C insertion products have been reported for platinum, and even fewer for palladium. Jones and colleagues pioneered the field and used nickel(0), palladium(0), and platinum(0) phosphine complexes for the activation of

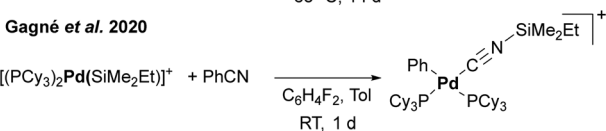
biphenylene (Scheme 1a),<sup>7–12</sup> as well as the photochemical activation of diphenylacetylene.<sup>13</sup> The insertion of the palladium(0) complex into biphenylene proceeded in reasonable yield only upon heating to 68 °C for 14 days.<sup>10,12,14</sup> Even for Ni(NHC)<sub>2</sub>, only a yield of 66% was obtained after stirring overnight.<sup>15,16</sup> The oxidative addition of benzonitrile with a bond dissociation energy (BDE) of 555 kJ mol<sup>−1</sup>, which considerably exceeds the one of the Ph–F bond (BDE = 485 kJ mol<sup>−1</sup>),<sup>17</sup> seems even more challenging.<sup>11,18</sup> Thus, it requires in the case of palladium the addition of Lewis-acids such as BEt<sub>3</sub><sup>19</sup> or silylium cations as studied by Gagné and coworkers (Scheme 1b).<sup>20,21</sup>

### Previously reported:

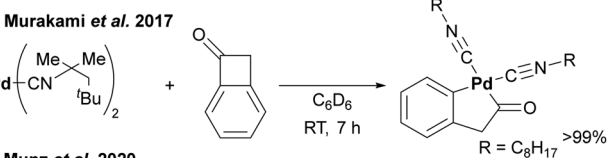
#### a) Jones *et al.* 1998



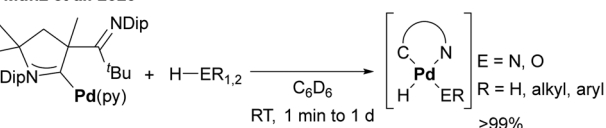
#### b) Gagné *et al.* 2020



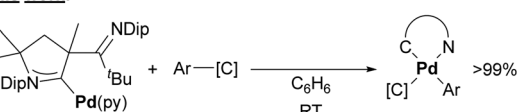
#### c) Murakami *et al.* 2017



#### d) Munz *et al.* 2020



### This work:



**Scheme 1** Insertion into C–C and H–E (E = N, O) bonds by palladium(0) complexes.

<sup>a</sup> Coordination Chemistry, Saarland University, Campus C4.1, Saarbrücken D-66123, Germany. E-mail: dominik.munz@uni-saarland.de

<sup>b</sup> Friedrich-Alexander-Universität Erlangen-Nürnberg, Inorganic and General Chemistry, Egerlandstr. 1, Erlangen D-91058, Germany

† Electronic supplementary information (ESI) available. CCDC 2288556–2288560. For ESI and crystallographic data in CIF or other electronic format see DOI: <https://doi.org/10.1039/d3cc03964a>



The C–C insertion of benzocyclopropene and naphtho[*b*]cyclopropene with  $(\text{PEt}_3)\text{Ni}(\text{COD})^{22,23}$  and  $(\text{PPh}_3)_2\text{Pt}(\text{C}_2\text{H}_4)^{24}$  have been studied as well, yet the products obtained with palladium proved unstable. Notwithstanding this, Murakami and coworkers isolated the insertion product of benzocyclobutenone with a palladium(0) complex bearing sterically hindered isocyanide ligands (Scheme 1c).<sup>25</sup> We reported a palladium(0) cyclic (alkyl)(amino) carbene (CAAC)<sup>26–30</sup> complex (**1**) with a labile pyridine ligand, which renders this complex a surrogate for monocoordinated 12-electron palladium(0).<sup>27,31</sup> This complex serves as precursor for exceedingly reactive nitrene complexes<sup>32–34</sup> and homolytically cleaves O–H and N–H bonds, whereby the hemilabile imino group allows to trap the transient Pd-hydrido species (Scheme 1d).<sup>35</sup> Thus, we reasoned that the softness of the palladium(0) metal center should also allow for the insertion into C–C bonds under unprecedented mild conditions.

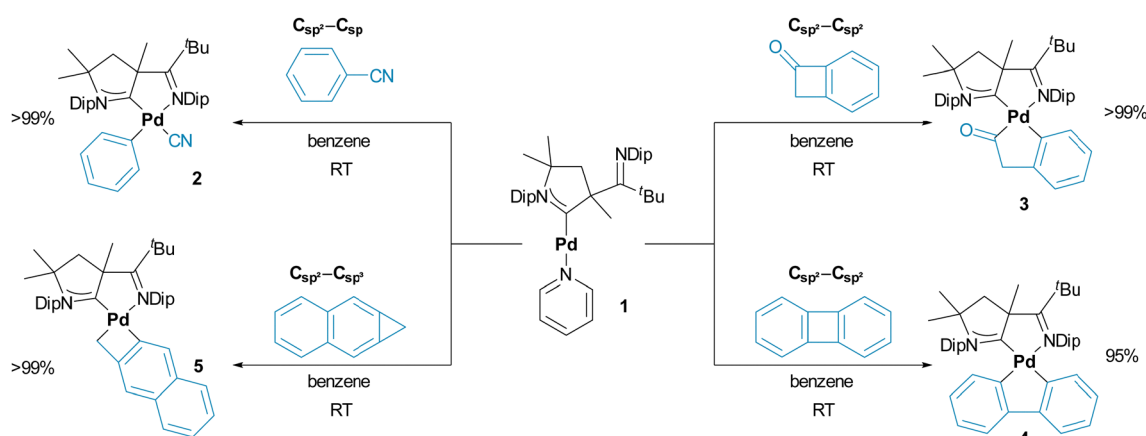
Indeed, treating dark-red **1** in benzene with equimolar equivalents (or a small excess of 1.1 to 1.5 eq.) of either benzonitrile (**2**), benzocyclobutenone (**3**), biphenylene (**4**), or naphtho[*b*]cyclopropene (**5**) led to an instantaneous color change from red to yellow/orange, which is indicative for the formation of palladium(II) (Scheme 2). Further, yellow precipitates/crystals started to form immediately. Compounds **3** and **5** crystallized quantitatively within 3–24 hours, whereas **2** and **4** required the addition of pentane in the workup. Running the reactions in thawing benzene likewise led to an immediate color-change and quantitative conversion within <5 min according to the *in situ* <sup>1</sup>H spectroscopic analysis. An exception is **2**, where  $\approx 4$  h are required (Fig. S6, ESI<sup>†</sup>). As expected, all these reactions take considerably longer in coordinating pyridine-*d*<sub>5</sub>, as illustrated by a reaction time of  $\approx 4$  days for **2**. Thereby, the *in situ* <sup>1</sup>H-NMR spectroscopic analysis (see Fig. S7 for C<sub>6</sub>D<sub>6</sub>, ESI<sup>†</sup>) reveals an intermediate, which we propose to be the  $\eta^2$ -coordinate  $\pi$ -complex.<sup>35</sup>

Single crystals suitable for XRD analysis were obtained directly from the reaction in case of **3** and **5**, *via* slow evaporation of a concentrated solution of **2** in pyridine, or through diffusion techniques (pentane/pyridine) at  $-30$  °C for **4** (Fig. 1). Comparing the bond lengths of the Pd–C<sub>Ar</sub> bonds between the

four complexes reveals remarkable *trans* influences. For **4**, the Pd–C bond *trans* to the CAAC is exceedingly long with 2.085(4) Å. In contrast, the other Pd–Ar bond is much shorter with 1.990(4) Å, and thus in the common range for palladium(II) phenyl complexes. Likewise, an elongated Pd–Ar bond of 2.085(2) Å was found in single crystals of **3**. Likely due to the constraints of the four-membered ring, this bond is moderately shorter (2.049(7) Å) in **5**, yet still unusually long in respect to common palladium phenyl compounds. The torsion angles between the CAAC and the aryl rings are also noteworthy. While this angle is large for **4** (N1–C1–C37–C42, 76.3°) and **3** (N2–C1–C36–C35, 39.3°), it is more acute for **5** (N2–C1–C38–C39, 18.9°). As a result, **5** features better spatial overlap between the aromatic  $\pi$ -system of the aryl ligand and the metal ion as well as the vacant p(z)-orbital of the carbene, which results in a short Pd–C<sub>carbene</sub> bond of only 2.011(7) Å.

In the case of **2**, this bond is even shorter with 1.9847(17) Å due to the *trans*-influence of the cyanido ligand. The palladacycles **4** and **5** are almost planar with the sum of the internal angles being close to the ideal (**4**, 538.5° *vs.* 540°; **5**, 359.2° *vs.* 360°). In contrast, palladacycle **3** is significantly bent (522.2° *vs.* 540°) and the carbonyl group is twisted out of plane with a short distance of approximately 3.1 Å to the mean plane of the phenyl ring of the diisopropylphenyl group. Small inter-ligand distances are also found for the phenylene groups in **3** and **4**. These palladacycle–CAAC interactions parallel the stability of complexes **3**, **4** and **5**. While **5** is perfectly stable in pyridine, solutions of **4** turn colorless within 2 h, thereby depositing insoluble needles. SC-XRD analysis identified these crystals as the di(pyridine) complex **6** (Fig. 2). In case of **3**, this transformation requires heating to 80 °C overnight (ESI<sup>†</sup>). Substitution reactions of CAACs are very unusual, and Pd<sup>II</sup>(CAAC) complexes are usually inert towards strong nucleophiles, including phosphines and other carbene-ligands.<sup>36,37</sup> We therefore propose that the loss of the CAAC ligand is due to steric congestion.

The ease of C–C activation may be understood by the interplay of ring strain and carbon atom hybridization. No ring strain is required for the oxidative addition into the C<sub>sp</sub><sup>2</sup>–C<sub>sp</sub> bond of benzonitrile (**2**) despite the high BDE of 555 kJ mol<sup>–1</sup>.<sup>11</sup> Although lower *s*-character of the C–C bond reduces the BDE



Scheme 2 Insertion of complex **1** into C<sub>sp</sub><sup>2</sup>–C<sub>sp</sub>, C<sub>sp</sub><sup>2</sup>–C<sub>sp</sub><sup>2</sup> and C<sub>sp</sub><sup>2</sup>–C<sub>sp</sub><sup>3</sup> bonds.





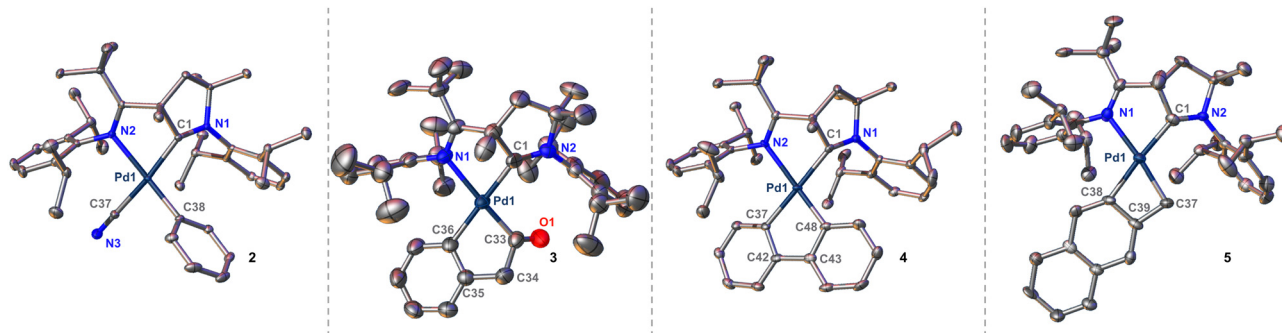


**Fig. 1** Solid state structures of complexes **2**, **3**, **4** and **5**. Thermal ellipsoids are shown at 50% probability. Hydrogen atoms and co-crystallized solvent molecules are omitted for clarity. Selected bond lengths [Å] and (torsion) angles [°]: **2**: Pd1–N2, 2.1846(14); Pd1–C1, 1.9847(17); Pd1–C37, 2.0182(18); Pd1–C38, 2.0107(17). **3**: Pd1–N1, 2.2460(15); Pd1–C1, 2.0565(18); Pd1–C33, 1.970(2); Pd1–C36, 2.0859(19); N2–C1–C36–C35, 39.3. **4**: Pd1–N2, 2.210(4); Pd1–C1, 2.044(4); Pd1–C37, 2.085(4); Pd1–C48, 1.990(4); N1–C1–C37–C42, 76.3. **5**: Pd1–N1, 2.175(6); Pd1–C1, 2.011(7); Pd1–C37, 2.062(6); Pd1–C38, 2.049(7); N2–C1–C38–C39, 18.9.

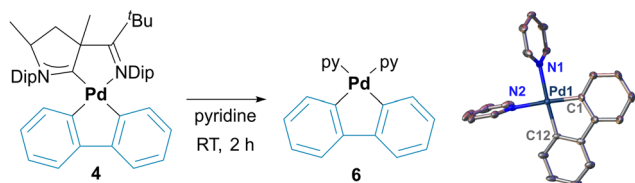


**Fig. 2** Solid state structures for the di(pyridine) complexes **6**. Thermal ellipsoids at 50% probability. Hydrogen atoms and co-crystallized solvent molecules are omitted for clarity. Selected bond lengths [Å]: Pd1–N1, 2.127(3); Pd1–N2, 2.128(3); Pd1–C1, 2.002(3); Pd1–C12, 2.002(3).

(Ph–Ph, BDE = 418 kJ mol<sup>-1</sup>),<sup>17</sup> it renders these compounds kinetically more stable (*vide infra*). As such, ring strain is required (**3**, computed at 116 kJ mol<sup>-1</sup>, Table S2; **4**,<sup>38</sup> 222 kJ mol<sup>-1</sup>) for the oxidative addition. In the case of **3**, selective insertion into C(O)–C<sub>sp</sub><sup>2</sup> was obtained, although the C(O)–C<sub>sp</sub><sup>3</sup> bond (CH<sub>3</sub>C(O)–Et, BDE = 349 kJ mol<sup>-1</sup> vs. CH<sub>3</sub>C(O)–Ph, BDE = 413 kJ mol<sup>-1</sup>)<sup>39</sup> is weaker. Compound **5** showcases that even C<sub>sp</sub><sup>3</sup>–C<sub>sp</sub><sup>2</sup> bonds (Ph–Et, BDE = 427.6 kJ mol<sup>-1</sup>)<sup>39</sup> may be activated in the presence of substantial ring-strain (computed at 291 kJ mol<sup>-1</sup>, Table S2 (ESI<sup>†</sup>); literature values benzocyclopropenes, 285–300 kJ mol<sup>-1</sup>).<sup>40</sup> Indeed, we did not observe a room-temperature reaction with benzocyclobutene, which features a C<sub>sp</sub><sup>3</sup>–C<sub>sp</sub><sup>2</sup> bond with a considerably reduced strain of 136 kJ mol<sup>-1</sup>.<sup>40</sup>

It is intriguing to note that the observed reactivity aligns with computational predictions by Ananikov, Musaev, and Morokuma.<sup>41</sup> Based on the calculation of oxidative addition transition states for CH<sub>3</sub>–CH<sub>3</sub>, Ph–Ph and HC<sub>2</sub>–C<sub>2</sub>H with Pd(PMe<sub>3</sub>)<sub>2</sub>, the authors proposed that low barriers, *viz.* fast reactions, are due to enhanced s-character in the transition state. The BDEs of the Pd–R and C–C bonds, which *both* follow the trend HC<sub>2</sub> > Ph > CH<sub>3</sub>, play a secondary role in the Bell–Evans–Polanyi (Hammond’s postulate, respectively) sense. It was furthermore shown that ground state inhibition through the formation of π-complexes in the case of olefins and especially alkynes somehow compromises this general trend. This

matches perfectly with the slow formation of **2** pending the formation of an intermediate (*vide supra*). We furthermore would like to highlight that the reactivity trend also coincides with the oxidative addition of organic (pseudo)halides, which has been attributed to both the higher stability of the forming Pd–C bonds as well as π-backbonding.<sup>42</sup>

In summary, we present the oxidative addition of biphenylene, benzonitrile, naphtho[*b*]cyclopropene, and benzocyclobutene to a palladium(0) complex. These insertion reactions proceed swiftly in (cold) benzene and, hence, under unprecedented mild conditions. Further, we report that complex **4** undergoes the unusual substitution of the CAAC ligand in pyridine. The ease of C–C bond insertion correlates with ring-strain and hybridization. Current efforts are targeting catalysis with stronger C–C bonds at elevated temperatures.

K.B.; investigation (synthesis and characterization **3**, **5** and **6**, computations), formal analysis, visualization, writing – original draft. A.G.; investigation (synthesis **2** and **4**). P.M.; characterization **4** and determination of all reaction times (investigation). F.D., crystallographic analysis **3**, **5** (investigation), contribution to writing – original draft; F.W.H. crystallographic analysis **2**, **4**, **6** (investigation). D.M.; conceptualization, funding acquisition, project administration, supervision, writing – review and editing.

This project has received funding from the European Research Council (ERC) under the European Union’s Horizon 2020 Research and Innovation Program (grant no. 948185). Instrumentation and technical assistance for the XRD analysis of **2** and **4** were provided by the Service Center X-ray Diffraction, with financial support from Saarland University and the German Science Foundation (DFG) (Project INST 256/506-1). We thank Peter Chen for providing a sample of naphtho[*b*]cyclopropene and N. Marigo for the preparation of starting materials. We also thank the Friedrich-Alexander-Universität Erlangen-Nürnberg (FAU) for generous financial support.

## Conflicts of interest

There are no conflicts to declare.



## Notes and references

- For reviews, see: (a) B. Rybtchinski and D. Milstein, *Angew. Chem., Int. Ed.*, 1999, **38**, 870–883; (b) F. Chen, T. Wang and N. Jiao, *Chem. Rev.*, 2014, **114**, 8613–8661; (c) L. Souillart and N. Cramer, *Chem. Rev.*, 2015, **115**, 9410–9464; (d) M. Murakami and N. Ishida, *J. Am. Chem. Soc.*, 2016, **138**, 13759–13769; (e) T. Kondo, *Eur. J. Org. Chem.*, 2016, 1232–1242; (f) G. Fumagalli, S. Stanton and J. F. Bower, *Chem. Rev.*, 2017, **117**, 9404–9432; (g) P. H. Chen, B. A. Billett, T. Tsukamoto and G. Dong, *ACS Catal.*, 2017, **7**, 1340–1360; (h) R. Vicente, *Chem. Rev.*, 2021, **121**, 162–226; (i) A. P. Y. Chan and A. G. Sergeev, *Coord. Chem. Rev.*, 2020, **413**, 213213; (j) G. Dong, C–C Bond Activation, *Top. Curr. Chem.*, 346, Springer, Berlin, Heidelberg, 2014; (k) M. Murakami and N. Chatani, *Cleavage of Carbon-Carbon Single Bonds by Transition Metals*, Wiley-VCH, Weinheim, Germany, 2015; for highlights, see: (l) S. Hu, T. Shima and Z. Hou, *Nature*, 2014, **512**, 413–415; (m) A. Sattler and G. Parkin, *Nature*, 2010, **463**, 523–526; (n) M. Jakoobi, Y. Tian, R. Boulatov and A. G. Sergeev, *J. Am. Chem. Soc.*, 2019, **141**, 6048–6053; (o) M. Jakoobi, N. Halcovitch, G. F. Whitehead and A. G. Sergeev, *Angew. Chem., Int. Ed.*, 2017, **56**, 3266–3269.
- T. Seiser and N. Cramer, *J. Am. Chem. Soc.*, 2010, **132**, 5340–5341.
- X. Fang, P. Yu and B. Morandi, *Science*, 2016, **351**, 832–836.
- C. Perthuisot, B. L. Edelbach, D. L. Zubris, N. Simhai, C. N. Iverson, C. Müller, T. Satoh and W. D. Jones, *J. Mol. Catal. A: Chem.*, 2002, **189**, 157–168.
- B. D. Swartz, W. W. Brennessel and W. D. Jones, *Organometallics*, 2011, **30**, 1523–1529.
- M. L. G. Sansores-Paredes, S. van der Voort, M. Lutz and M.-E. Moret, *Angew. Chem., Int. Ed.*, 2021, **60**, 26518–26522.
- B. L. Edelbach, R. J. Lachicotte and W. D. Jones, *Organometallics*, 1999, **18**, 4040–4049.
- N. Simhai, C. N. Iverson, B. L. Edelbach and W. D. Jones, *Organometallics*, 2001, **20**, 2759–2766.
- C. Müller, R. J. Lachicotte and W. D. Jones, *Organometallics*, 2002, **21**, 1975–1981.
- J. J. Garcia and W. D. Jones, *Organometallics*, 2000, **19**, 5544–5545.
- J. J. Garcia, N. M. Brunkan and W. D. Jones, *J. Am. Chem. Soc.*, 2002, **124**, 9547–9555.
- B. L. Edelbach, R. J. Lachicotte and W. D. Jones, *J. Am. Chem. Soc.*, 1998, **120**, 2843–2853.
- C. Müller, C. N. Iverson, R. J. Lachicotte and W. D. Jones, *J. Am. Chem. Soc.*, 2001, **123**, 9718–9719.
- B. L. Edelbach, D. A. Vivic, R. J. Lachicotte and W. D. Jones, *Organometallics*, 1998, **17**, 4784–4794.
- T. Schaub and U. Radius, *Chem. – Eur. J.*, 2005, **11**, 5024–5030.
- T. Schaub, M. Backes and U. Radius, *Organometallics*, 2006, **25**, 4196–4206.
- J. A. Dean, *Lange's Handbook of Chemistry*, McGraw-Hill, INC., New York St. Louis San Francisco Auckland Bogotá Caracas Lisbon London Madrid Mexico Milan Montreal New Delhi Paris San Juan São Paulo Singapore Sydney Tokyo Toronto, 15th edn, 1999.
- S. Lachaize, D. C. Gallegos, J. J. Antonio, A. C. Atesin, T. A. Ateşin and W. D. Jones, *Organometallics*, 2023, **42**, 2134–2147.
- L. Munjanja, C. Torres-López, W. W. Brennessel and W. D. Jones, *Organometallics*, 2016, **35**, 2010–2013.
- A. L. Wierschen, J. Lowe, N. Romano, S. J. Lee and M. R. Gagné, *Organometallics*, 2020, **39**, 1258–1268.
- A. L. Wierschen, N. Romano, S. J. Lee and M. R. Gagne, *J. Am. Chem. Soc.*, 2019, **141**, 16024–16032.
- R. Neidlein, A. Ruffińska, H. Schwager and G. Wilke, *Angew. Chem., Int. Ed. Engl.*, 1986, **25**, 640–642.
- C. Krüger, K. Laakmann, G. Schroth, H. Schwager and G. Wilke, *Chem. Ber.*, 2006, **120**, 471–475.
- P. J. Stang, L. Song and B. Halton, *J. Organomet. Chem.*, 1990, **388**, 215–220.
- S. Okumura, F. Sun, N. Ishida and M. Murakami, *J. Am. Chem. Soc.*, 2017, **139**, 12414–12417.
- V. Lavallo, Y. Canac, C. Präsang, B. Donnadiou and G. Bertrand, *Angew. Chem., Int. Ed.*, 2005, **44**, 5705–5709.
- J. Chu, D. Munz, R. Jazzar, M. Melaimi and G. Bertrand, *J. Am. Chem. Soc.*, 2016, **138**, 7884–7887.
- M. Melaimi, R. Jazzar, M. Soleilhavoup and G. Bertrand, *Angew. Chem., Int. Ed.*, 2017, **56**, 10046–10068.
- F. Vermersch, L. Oliveira, J. Hunter, M. Soleilhavoup, R. Jazzar and G. Bertrand, *J. Org. Chem.*, 2022, **87**, 3511–3518.
- K. Breitwieser and D. Munz, *Adv. Organomet. Chem.*, 2022, **78**, 79–132.
- D. Munz, J. Chu, M. Melaimi and G. Bertrand, *Angew. Chem., Int. Ed.*, 2016, **55**, 12886–12890.
- A. Grünwald, B. Goswami, K. Breitwieser, B. Morgenstern, M. Gimferrer, F. W. Heinemann, D. M. Momper, C. W. M. Kay and D. Munz, *J. Am. Chem. Soc.*, 2022, **144**, 8897–8901.
- S. J. Goodner, A. Grünwald, F. W. Heinemann and D. Munz, *Aust. J. Chem.*, 2019, **72**, 900–903.
- A. Grünwald, N. Orth, A. Scheurer, F. W. Heinemann, A. Pöthig and D. Munz, *Angew. Chem., Int. Ed.*, 2018, **57**, 16228–16232.
- A. Grünwald, F. W. Heinemann and D. Munz, *Angew. Chem., Int. Ed.*, 2020, **59**, 21088–21095.
- E. Tomás-Mendivil, M. M. Hansmann, C. M. Weinstein, R. Jazzar, M. Melaimi and G. Bertrand, *J. Am. Chem. Soc.*, 2017, **139**, 7753–7756.
- N. Marigo, B. Morgenstern, A. Biffis and D. Munz, *Organometallics*, 2023, **42**, 1567–1572.
- I. Novak, *J. Phys. Chem. A*, 2008, **112**, 2503–2506.
- S. J. Blanksby and G. B. Ellison, *Acc. Chem. Res.*, 2003, **36**, 255–263.
- R. Benassi, S. Ianelli, M. Nardelli and F. Taddei, *J. Chem. Soc., Perkin Trans. 2*, 1991, 1381–1386.
- V. P. Ananikov, D. G. Musaev and K. Morokuma, *Organometallics*, 2005, **24**, 715–723.
- A. Ariafard and Z. Lin, *Organometallics*, 2006, **25**, 4030–4033.

